JOURNAL OF MAGNETIC RESONANCE, Series B 101, 210–213 (1993)

Increased Resolution and Improved Spectral Quality in Four-Dimensional $^{13}C/^{13}C$-Separated HMQC–NOESY–HMQC Spectra Using Pulsed Field Gradients

GEERTEN W. VUISTER, G. MARIUS CLORE, ANGELA M. GRONENBORN, ROBERT POWERS, DANIEL S. GARRETT, ROLF TSCHUDIN, AND AD BAX

Laboratory of Chemical Physics, National Institutes of Diabetes and Digestive and Kidney Diseases, National Institutes of Health, Bethesda, Maryland 20892

Received November 25, 1992

Pulsed field gradients (PFG) make it possible to record two- and three-dimensional spectra using experiments with only a single scan per increment (*1–10*). In these experiments PFGs are employed to select the desired coherence-transfer pathway. However, each time a combination of PFGs is used to select a coherence transfer from order n to m, a second desired pathway, from $-n$ to m, is eliminated, resulting in an intrinsic sensitivity loss of a factor $\sqrt{2}$. Consequently, coherence pathway selection by means of PFGs is suitable only for applications where the signal-to-noise ratio is not a limiting factor. However, for 3D and 4D experiments applied to dilute protein samples, the intrinsic loss in signal-to-noise of $\sqrt{2}$ for each PFG coherence selection step is highly undesirable. To circumvent this problem, a different strategy which relies on suppression of undesired coherence-transfer pathways can be used (*11*). In this latter approach, coherences associated with spurious magnetization transfer, which frequently result from pulse imperfections, can be eliminated, thereby reducing the number of phase-cycling steps required. A shorter phase cycle allows a reduction in measuring time for experiments that are not limited by the signal-to-noise ratio. Alternatively, it permits an increase in resolution in the indirectly detected dimensions of experiments where measuring time limits the number of increments that can be executed.

Heteronuclear 3D and 4D J correlation techniques make it possible to obtain complete ^1H, ^{13}C, and ^{15}N resonance assignments for uniformly $^{13}C/^{15}N$-enriched proteins of up to several hundred amino acids (*12, 13*). Measurement of ^1H–^1H NOEs, however, constitutes the basis for the protein structure determination process and both the precision and the accuracy of the resulting structures are directly related to the number of unambiguously determined NOEs (*14, 15*). For uniformly $^{13}C/^{15}N$-enriched proteins, the 4D $^{13}C/^{15}N$-separated NOESY (*16*) and the $^{13}C/^{13}C$-separated NOESY (*17, 18*) experiments are the methods of choice since they provide the highest possible dispersion of resonances. In the corresponding 4D spectra, ^1H–^1H NOE cross peaks are separated in a third dimension by the frequency of the heteroatom attached to the first proton and in a fourth dimension by the frequency of the heteroatom attached to the second proton. Resolution in the heteronuclear dimensions of these 4D experiments typically has been limited by the fact that only eight complex points could be acquired in these dimensions, corresponding to very short acquisition times, on the order of a few milliseconds. Longer acquisition times, combined with the required extensive phase cycling, would result in unacceptably long measuring times. For the 4D $^{13}C/^{13}C$-separated HMQC–NOESY–HMQC experiment, the artifacts resulting from spurious magnetization-transfer pathways associated with the strong diagonal resonances in the spectrum were a major consideration in the design of the previously proposed eight-step phase cycle (*17*). This phase cycle is a compromise in which several noninteracting phase cycles are executed simultaneously. In addition, two trim pulses are needed to further reduce artifacts. In contrast, as will be demonstrated below, the gradient version of the 4D $^{13}C/^{13}C$-separated HMQC–NOESY–HMQC experiment does not lower the signal-to-noise ratio and requires only a two-step phase cycle that results in spectra with reduced artifacts and increased resolution.

The pulse scheme for the gradient version of the 4D $^{13}C/^{13}C$-separated HMQC–NOESY–HMQC experiment is shown in Fig. 1A. Because the experiment consists of simple building blocks that have extensively been discussed before (*16–18*), only the fate of some undesired coherences will be discussed, as these provide the rationale for the choice of the gradient pulses. In the following discussion, the spin operators I and S denote the coupled ^1H and ^{13}C spins.

The effects of the imperfection of a 180° refocusing pulse on transverse spin operators can be removed by the application of PFGs of identical strength and polarity at either side of this pulse (*11*). Both the set of PFGs labeled G_1 and the set labeled G_4 in Fig. 1A are used for this purpose. As

1064-1866/93 $5.00

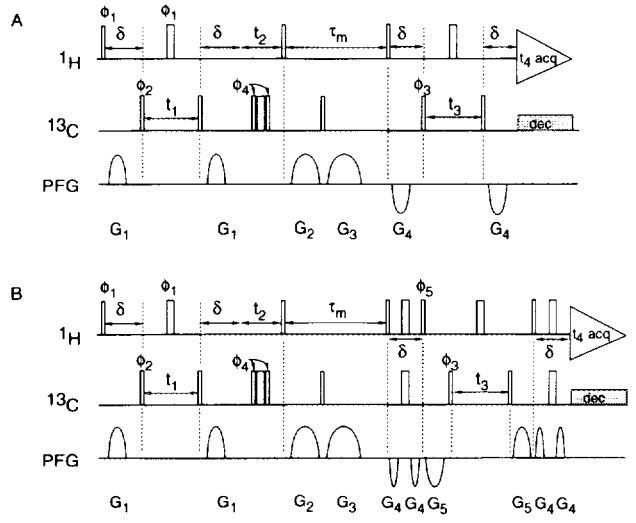

FIG. 1. Pulse schemes for the gradient versions of the 4D $^{13}C/^{13}C$-separated HMQC-NOESY-HMQC (A) and HMQC-NOESY-HSQC (B) experiments. Narrow and wide pulses denote 90° and 180° flip angles, respectively. Unless indicated otherwise, all pulses are applied along the x axis. A two-step phase cycle is used: $\phi_1 = x$; $\phi_2 = x, -x$; $\phi_3 = x$; $\phi_4 = y$; $\phi_5 = y$; receiver $= x, -x$. Quadrature detection in t_1, t_2, and t_3 is obtained with the States-TPPI method (*20*), incrementing independently the phases ϕ_2, ϕ_1, and ϕ_3, respectively. Sine-bell-shaped pulsed field gradients (PFG) with a strength of 7 G/cm at their maximum are applied along the z axis. Gradients used have the following durations: $G_1 = 750$ μs, $G_2 = 2$ ms, $G_3 = 4$ ms, $G_4 = 750$ μs (negative polarity). The delay δ is set to 3.5 ms and ^{13}C decoupling during ^{1}H data acquisition is accomplished with a GARP decoupling scheme (*21*), using an RF field strength of 4.5 kHz.

the G_4 PFGs are applied before and after the t_3 period, evolution of the ^{13}C spin operators during t_3 is not affected. Note, however, that the $\sin(\Omega_C t_3)$ fraction of the ^{13}C magnetization, which remains as multiple-quantum coherence after the last ^{13}C 90° pulse, is defocused by the last G_4 PFG. When not eliminated, this residual multiple-quantum coherence can give rise to significant decoupling modulation sidebands during the time t_4 (*19*). The effects of a nonideal 180° ^{1}H pulse in the center of the t_1 period are eliminated in the same way as that described above for the last 180° ^{1}H pulse.

Although, at the end of the t_2 evolution period, most ^{1}H magnetization is in-phase with respect to its attached ^{13}C, a small fraction remains antiphase because (a) for sensitivity reasons the delay δ is usually kept slightly shorter than $1/(2J_{CH})$, and (b) not all ^{13}C spins are inverted by the composite 180° ^{13}C pulse applied at the midpoint of t_2. As a consequence, the second 90° ^{1}H pulse, applied at the start of the NOESY mixing period, can generate a small amount of I_zS_z order. At the end of the NOE mixing period, a fraction of this two-spin order could be converted by the remainder of the pulse sequence into spurious magnetization observable during the time t_4. It is therefore necessary to eliminate this type of zz order during the NOE mixing period, together with all transverse magnetization components. This is accomplished by the application of the gradient G_2 (for the transverse terms), followed by a 90° ^{13}C pulse and a subsequent gradient G_3 for eliminating the I_zS_z order. Although the polarities of G_1 and G_4 relative to G_2 and G_3 can be choosen arbitrarily, G_1 and G_4 have opposite signs in order to minimize the disturbance of the deuterium lock.

The gradients used in the 4D $^{13}C/^{13}C$-separated HMQC-NOESY-HMQC experiment are applied either during delays that are needed for dephasing and rephasing of transverse magnetization or during the NOE mixing period. Therefore, no additional delays are required for the application of the gradient pulses. Although the gradients used are relatively weak (7 G/cm), their required duration is much shorter than the dephasing and rephasing periods, δ.

In the absence of any phase cycling, the pulse scheme of Fig. 1A does not eliminate the signals from protons not attached to ^{13}C, resulting in axial resonances in both the F_1 and the F_3 dimensions of the 4D spectrum. Removal of these axial peaks requires selection of the desired heteronuclear coherence-transfer pathways during t_1 and t_3 by means of PFGs (*1–10*), purging of signals from protons not attached to ^{13}C, or additional phase cycling. We have chosen the last option, using a $\pm x$ phase cycle of the first 90° ^{13}C pulse, together with a $\pm x$ phase cycle for the receiver. Because no such heteronuclear filtering is used after the NOESY mixing period, axial peaks, shifted to the edge of the spectrum in the F_3 dimension by the States-TPPI procedure (*20*), are present in the 4D spectrum. Fortunately, their intensities are weak as they result from the small fraction ($<\sim 10\%$) of magnetization that is converted into multiple-quantum coherence during the time t_1, but that is not converted during the time t_3. Signals from protons not attached to ^{13}C, such as the residual HDO signal, and signals originating from longitudinal relaxation during the NOE mixing period are effectively removed by the two-step phase cycle. However, for cases where the ^{13}C enrichment is incomplete, or for the study of a complex between an unlabeled ligand and a labeled protein, an additional $\pm x$ phase-cycling step is required for one of the 90° pulses of the last HMQC transfer, resulting in a four-step phase cycle for the 4D experiment. Alternatively, these signals may be removed by using an HSQC- instead of an HMQC-type ^{1}H–^{13}C correlation after the NOESY mixing period (Fig. 1B), which allows for suppression of ^{1}H coherence during the two INEPT stages of this experiment (*11*), without resorting to a four-step phase cycle. However, the sensitivity of the scheme in Fig. 1B was found to be lower than that of the scheme in Fig. 1A, mainly due to the additional 180° pulses in the HSQC type of correlation, which are far from ideal near the edges of the ^{1}H and ^{13}C spectrum. Indeed, the loss in sensitivity is largest for interactions to methyl and aromatic protons. Therefore, we found the scheme in Fig. 1A preferable, using only a two-step phase cycle. For this experiment, the residual axial peaks at the edges of the ^{13}C (F_3) spectral window can obscure the NOE

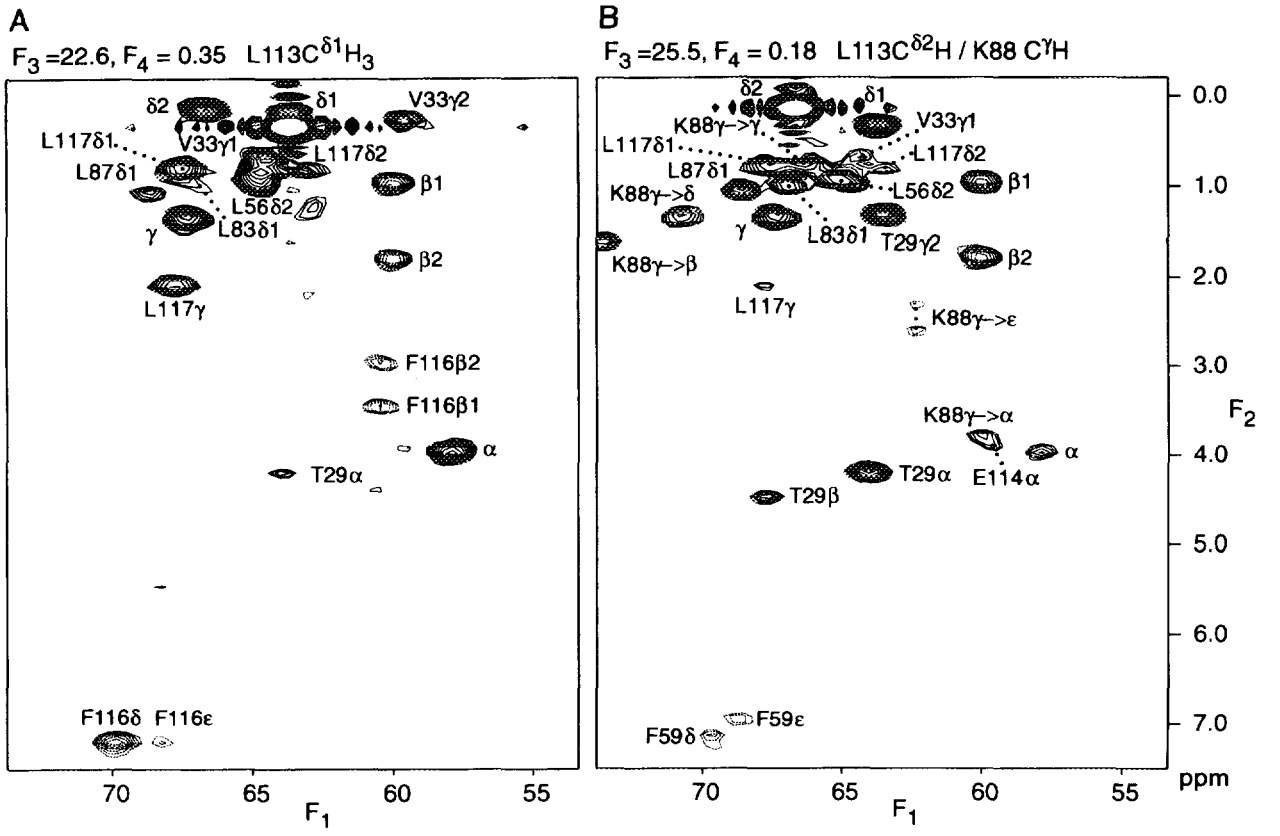

FIG. 2. (F_1, F_2) cross sections through the 4D $^{13}C/^{13}C$-separated 4D NOESY spectrum of IL-4, recorded with a 107 ms NOE mixing time. Cross sections shown are taken at the F_3/F_4 ($^{13}C/^{1}H$) resonance frequencies of (A) Leu113-$C^{\delta 1}H_3$ and (B) the partially overlapping correlations of Leu113-$C^{\delta 2}H_3$ and Lys88-$C^{\gamma}H_2$. These cross sections display the ^{1}H-^{13}C correlations for all protons that have an NOE interaction with (A) Leu113-$C^{\delta 1}H_3$ and (B) Leu113-$C^{\delta 2}H_3$ or Lys88-$C^{\gamma}H_2$. For intraresidue cross peaks, the residue designation has been omitted from the cross-peak label. The spectrum results from a dataset of $18^*(t_1) \times 64^*(t_2) \times 16^*(t_3) \times 300^*(t_4)$, where n^* denotes n complex points, with acquisition times 5.76, 11.9, 5.12, and 49.8 ms, respectively. Total measuring time was 84 h. Data were processed using in-house written routines for all four dimensions. Data were apodized by a 72°-shifted squared sine-bell window in t_4 and zero-filled to 512* prior to Fourier transformation and phasing. In t_2, the data were apodized by a 81°-shifted sine-bell window, zero-filled to 128*, and Fourier transformed. Finally, in both the t_1 and the t_3 domains, 75°-shifted sine-bell windows were used, followed by zero-filling to 64*, Fourier transformation, and phasing. The size of the absorptive part of the resulting data set was $64(t_1) \times 128(t_2) \times 64(t_3) \times 512(t_4)$. In practice, this large data set was processed in parts, splitting the data set in the F_4 dimension after the first Fourier transformation. The ^{1}H and ^{13}C carriers were placed at 3.98 and 63.7 ppm, respectively. Since the spectral width in the ^{13}C dimensions was adjusted to 3125 Hz (20.7 ppm) resonances are extensively folded in F_1 and F_3. The initial delays in t_1 and t_3 were chosen to assure a 90° zero-order and −180° first-order phase correction in these domains and therefore, depending on whether resonances have aliased an odd or even number of times, they appear as negative peaks (broken contours) or positive peaks (solid contours), respectively (*22*). Assignments are taken from Ref. (*23*).

correlation from a proton H_A to a proton H_B if its attached carbon, C_B, resonates close to the edge of the F_3 spectral window. However, its mirror image, corresponding to NOE transfer from H_B to H_A, will be clearly observable unless C_A also resonates close to the edge of the F_3 spectral window.

The experiment is demonstrated for a 1.7 m*M* solution of the protein interleukin-4 (IL-4) (~15.4 kDa), uniformly enriched (>95%) with ^{13}C and ^{15}N, dissolved in D_2O, pH 5.7. The experiment was recorded at 36°C on a Bruker AMX600, operating at a ^{1}H resonance frequency of 600.13 MHz. A Bruker triple-resonance probe equipped with a self-shielded *z* gradient was used, together with an in-house-developed gradient pulse-shaping unit and amplifier. Sine-bell-shaped gradient pulses had a strength of 7 G/cm at the center of the sine bell. To adjust different relative strengths of the PFGs, the durations and not the amplitudes of these pulses were varied.

Figure 2 shows two 2D cross sections taken through the 4D $^{13}C/^{13}C$-separated gradient-HMQC-NOESY-HMQC spectrum of IL-4, taken perpendicular to the F_3 (^{13}C) and F_4 (^{1}H) coordinates of the two C^{δ} methyl groups of Leu-113. These cross sections therefore show the frequencies of the protons (together with the chemical shifts of their attached ^{13}C nuclei) that have an NOE interaction to these two methyl groups. Several features deserve special note. First, the resolution in the ^{13}C (F_1) dimension is high for a 4D spectrum, permitting the unique identification of many NOEs in crowded parts of the spectrum, such as the methyl-

methyl region. For example, the structurally important NOE interactions between Leu113-$C^{\delta 1}H_3$ and Leu56-$C^{\delta 2}H_3$ or Leu83-$C^{\delta 1}H_3$ would be unresolvable with poorer resolution (Fig. 2A). Second, the level of artifacts is very low. Only some sinc wiggles resulting from truncation of the time-domain signal of the intense "diagonal resonance" of Leu113-$C^{\delta 1}H_3$ are observed. In fact, comparison between the 4D spectrum recorded with the previously published eight-step phase cycle (*17*) (data not shown) and the present data set indicates that the artifacts associated with the intense diagonal resonances are reduced nearly 10-fold. This low level of artifacts makes it possible to unambiguously identify the structurally important NOE between Leu113-$C^{\delta 1}H_3$ and Val33-$C^{\gamma}H_3$, despite the fact that the proton chemical shifts of these two methyl groups are nearly degenerate (Fig. 2A).

In Fig. 2B, NOEs to Leu113-$C^{\delta 2}H_3$ and Lys88-$C^{\gamma}H_2$ are shown in a cross section taken at (F_3, F_4) = (25.2, 0.18) ppm. As expected, many of the NOEs observed for Leu113-$C^{\delta 1}H_3$ in Fig. 2A are also observed for Leu113-$C^{\delta 2}H_3$. The cross section also shows intraresidue NOEs from the α, β, δ, and ϵ protons to the γ protons of Lys88. Interestingly, as a result of the high resolution in the F_3 dimension (perpendicular to the plane shown), the F_3 coordinates of the NOE cross peaks to Leu113-$C^{\delta 2}H_3$ and Lys88-$C^{\gamma}H_2$ are sufficiently different (0.3 ppm) to unambiguously establish the NOE between Leu113-$C^{\delta 2}H_3$ and Leu87-$C^{\delta 1}H_3$ and to exclude the possibility of an NOE from Lys88-$C^{\gamma}H_2$ to Leu87-$C^{\delta 1}H_3$.

Our results show that straightforward incorporation of PFGs in the 4D ^{13}C-separated HMQC-NOESY-HMQC experiment makes it possible to record high-quality 4D spectra with high resolution in all four frequency dimensions in a reasonable amount of measuring time (3.5 days). Incorporation of the PFGs does not decrease the sensitivity of the experiment but greatly reduces the level of spectral artifacts. Acquisition times in the ^{13}C dimensions of the 4D experiment much longer than the 5.7 ms used in the present case would degrade the signal-to-noise obtainable per unit of measuring time because the ^{13}C signal in these dimensions rapidly decreases as the acquisition times approach $1/(2J_{CC})$ ($\sim$14 ms). Consequently, the durations of the acquisition times in the t_1 and t_3 ^{13}C dimensions used in the present experiment are a good compromise between optimum sensitivity and maximum spectral resolution. In principle, it is possible to record the 4D spectrum without any phase cycling by replacing both HMQC elements by HSQC elements with appropriate PFGs. However, because of the signal losses associated with the larger number of RF pulses required for an HSQC-type correlation, the intrinsic sensitivity of the HSQC version of the experiment is somewhat lower than that of the HMQC version.

ACKNOWLEDGMENTS

We thank Frank Delaglio and Stephan Grzesiek for writing the processing software. This work was supported by a grant from the AIDS Targeted Anti-Viral Program of the Office of the Director of the National Institutes of Health (to G.M.C., A.M.G., and A.B.).

REFERENCES

1. A. Bax, P. G. de Jong, A. F. Mehlkopf, and J. Smidt, *Chem. Phys. Lett.* **69**, 567 (1980).
2. P. Barker and R. Freeman, *J. Magn. Reson.* **64**, 334 (1985).
3. R. E. Hurd, *J. Magn. Reson.* **87**, 422 (1987).
4. R. E. Hurd and B. K. John, *J. Magn. Reson.* **91**, 648 (1991).
5. R. E. Hurd and B. K. John, *J. Magn. Reson.* **92**, 658 (1991).
6. A. L. Davis, E. D. Laue, J. Keeler, D. Moskau, and J. Lohman, *J. Magn. Reson.* **94**, 637 (1991).
7. G. W. Vuister, R. Boelens, R. Kaptein, R. E. Hurd, B. John, and P. C. M. van Zijl, *J. Am. Chem. Soc.* **113**, 9688 (1991).
8. B. K. John, D. Plant, S. L. Heald, and R. E. Hurd, *J. Magn. Reson.* **94**, 664 (1991).
9. G. W. Vuister, R. Boelens, R. Kaptein, M. Burgering, and P. C. M. van Zijl, *J. Biomol. NMR* **2**, 301 (1992).
10. A. L. Davis, R. Boelens, and R. Kaptein, *J. Biomol. NMR* **2**, 395 (1992).
11. A. Bax and S. Pochapsky, *J. Magn. Reson.* **99**, 638 (1992).
12. G. M. Clore and A. M. Gronenborn, *Prog. NMR Spectrosc.* **23**, 43 (1991).
13. A. Bax and S. Grzesiek, *Acc. Chem. Res.*, in press.
14. G. M. Clore and A. M. Gronenborn, *Science* **252**, 1390 (1991).
15. Y. Liu, D. Zhao, R. Altman, and O. Jardetzky, *J. Biomol. NMR* **2**, 373 (1992).
16. L. E. Kay, G. M. Clore, A. Bax, and A. M. Gronenborn, *Science* **249**, 411 (1990).
17. G. M. Clore, L. E. Kay, A. Bax, and A. M. Gronenborn, *Biochemistry* **30**, 12 (1991).
18. E. R. P. Zuiderweg, A. M. Petros, S. W. Fesik, and E. T. Olejniczak, *J. Am. Chem. Soc.* **113**, 370 (1991).
19. A. Bax, G. M. Clore, P. C. Driscoll, A. M. Gronenborn, M. Ikura, and L. E. Kay, *J. Magn. Reson.* **87**, 620 (1990).
20. D. Marion, M. Ikura, R. Tschudin, and A. Bax, *J. Magn. Reson.* **85**, 393 (1989).
21. A. J. Shaka, P. Barker, and R. Freeman, *J. Magn. Reson.* **53**, 313 (1983).
22. A. Bax, M. Ikura, L. E. Kay, and G. Zhu, *J. Magn. Reson.* **91**, 174 (1991).
23. R. Powers, D. S. Garrett, C. J. March, E. A. Frieden, A. M. Gronenborn, and G. M. Clore, *Biochemistry* **31**, 4334 (1992).